

Minimum Disturbance Measurement without Post-Selection

So-Young Baek,^{1,*} Yong Wook Cheong,² and Yoon-Ho Kim^{1,†}

¹*Department of Physics, Pohang University of Science and Technology (POSTECH), Pohang, 790-784, Korea*

²*Department of Physics Education, Seoul National University, Seoul, 151-742, Korea*

(Revised: November 12, 2018)

We propose and demonstrate a linear optical device which deterministically performs optimal quantum measurement or minimum disturbance measurement on a single-photon polarization qubit with the help of an ancillary path qubit introduced to the same photon. We show theoretically and experimentally that this device satisfies the minimum disturbance measurement condition by investigating the relation between the information gain (estimation fidelity) and the state disturbance due to measurement (operation fidelity). Our implementation of minimum disturbance measurement is postselection-free in the sense that all detection events are counted toward evaluation of the estimation fidelity and the operation fidelity, i.e., there is no need for coincidence postselection of the detection events.

PACS numbers: 03.67.-a, 03.65.Wj, 42.50.Dv, 42.50.-p

A measurement is a process by which we learn about the observed system by interacting it with a measuring apparatus. The role of the measurement process is one of the most unique features that distinguish quantum physics from classical physics [1]. One of the fundamental aspects of the quantum measurement process is that the quantum state of the observed system is unavoidably altered by the measurement process itself which may be direct, as manifested in the Heisenberg's uncertainty principle [2], or indirect, as demonstrated in the quantum eraser-type test on the complementarity [3, 4].

Quantitative study of on the relation between the information gain by a measurement and the measurement-induced state disturbance is, obviously, a relevant and an important issue in quantum physics and quantum information [5]. In particular, how to achieve the optimal quantum measurement process, in which the information gain is maximal while the measurement-induced state disturbance is minimal, is an important fundamental as well as a practically relevant problem in quantum communication [6, 7, 8].

Recently, the trade-off relation between the information gain and the state disturbance was derived in the context of a finite d -dimensional quantum system by quantifying the information gain as the estimation fidelity and the state disturbance as the operation fidelity [9]. The measurement protocol which saturates the trade-off relation is known as the minimum disturbance measurement (MDM). Experimental demonstrations of MDM to date, however, have been rather limited. In Ref. [10], a MDM protocol was implemented for a single-photon polarization qubit with an ancilla single-photon polarization qubit by using classical active feed-forward and a linear optical nondeterministic quantum logic op-

eration based on coincidence postselection of detection events [11]. The scheme, therefore, is probabilistic in principle and post-selection of the final detection events is necessary. In Ref. [12], a MDM protocol was demonstrated for an infinite dimensional Gaussian state by using linear optics, amplitude and phase modulators, and homodyne detection. This scheme, therefore, applies to a coherent state but not to a qubit.

In this Letter, we propose and demonstrate a novel postselection-free linear optical MDM device which deterministically performs optimal quantum measurement of the polarization qubit of a single-photon. The ancilla qubit which interacts with the polarization qubit is the path qubit introduced to the same photon, i.e., our device makes use of the single-photon polarization-path two-qubit state [13]. We first show theoretically that this device performs minimum disturbance measurement by investigating the trade-off relation between the estimation fidelity and the operation fidelity. We then demonstrate that the experimental estimation and operation fidelities indeed closely follow the theoretical bound for MDM. Our MDM is postselection-free in the sense that all detection events are counted toward the evaluation of the operation and estimation fidelities. To the best of our knowledge, postselection-free MDM for a qubit has not been reported to date.

The quantum circuit for the proposed MDM scheme is shown in Fig. 1. The system qubit, which is to be

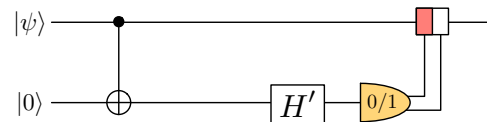


FIG. 1: Quantum circuit for the proposed MDM on the system qubit $|\psi\rangle$. H' is a Hadamard-like transformation on the ancilla qubit and controls the amount of information gain on the system qubit via measurement on the ancilla qubit.

*Electronic address: simply@postech.ac.kr

†Electronic address: yoonho@postech.ac.kr

measured, is prepared in an arbitrary quantum state $|\psi\rangle_s = \alpha|0\rangle_s + \beta|1\rangle_s$ with $|\alpha|^2 + |\beta|^2 = 1$. The ancilla qubit, initialized in the state $|0\rangle_a$, is introduced to make optimal measurement on the system qubit by interacting with it. The controlled-not (CNOT) operation between the system and the ancilla qubits transforms the initial two-qubit state $|\psi\rangle_s \otimes |0\rangle_a$ into $\alpha|0\rangle_s|0\rangle_a + \beta|1\rangle_s|1\rangle_a$, i.e., the system and the ancilla qubits are now entangled. The ancilla qubit then undergoes to the Hadamard-like unitary transformation $H' = \begin{pmatrix} t & r \\ r & -t \end{pmatrix}$. Here t and r satisfy the normalization condition $|t|^2 + |r|^2 = 1$ and we assume $|t| \geq |r|$ without loss of generality.

After the H' operation, the joint state of the system and the ancilla qubits is given as

$$(\alpha t|0\rangle_s + \beta r|1\rangle_s)|0\rangle_a + (\alpha r|0\rangle_s - \beta t|1\rangle_s)|1\rangle_a. \quad (1)$$

First, consider the case of $t = r$ which is equivalent to randomly guessing the state of the system qubit. If the ancilla measurement outcome is 0, the state of the system qubit is unchanged but if the ancilla measurement outcome is 1, it is necessary to apply the feed-forward σ_z operation to the system qubit, i.e., $|1\rangle_s \rightarrow -|1\rangle_s$, to recover the original quantum state. Next, consider the case of $t \neq r$. More information about the system qubit can be obtained at the expense of increased state disturbance. The quantum circuit in Fig. 1, therefore, allows us to vary the “strength” of the measurement on the system qubit with variables t and r , hence varying the amount of information we can gain about the system qubit from the measurement outcomes of the ancilla qubit.

To see if the quantum circuit in Fig. 1 satisfy the minimum disturbance condition in Ref. [9], it is necessary to investigate the relation between the estimation fidelity G and the operation fidelity F . Consider the state in eq. (1). The probabilities of ancilla measurement outcomes 0 and 1 are calculated to be $P_0 = |\alpha|^2 t^2 + |\beta|^2 r^2$ and $P_1 = |\alpha|^2 r^2 + |\beta|^2 t^2$, respectively. The state of the system qubit is then estimated to be $\rho_G = P_0|0\rangle_{ss}\langle 0| + P_1|1\rangle_{ss}\langle 1|$, i.e., when the measurement outcome of the ancilla qubit is i ($i = 0$ or 1), the system qubit is guessed to be in the state $|i\rangle_s$ with probability of P_i . The overlap between the the inferred (guessed) state of the system qubit ρ_G and the original state of the system qubit $|\psi\rangle_s$ is defined to be the estimation fidelity $G_\psi = {}_s\langle \psi | \rho_G | \psi \rangle_s$ and is dependent on the measurement strength controlled by H' . If we consider all possible pure states on the Bloch sphere as the system qubit, the average estimation fidelity is calculated to be

$$G_{\text{avg}} = \int G_\psi d\psi = \frac{1}{3}(t^2 + 1). \quad (2)$$

The state of the system qubit after the feed-forward operation in Fig. 1 can be evaluated by tracing over the Hilbert space of the ancilla qubit on the final

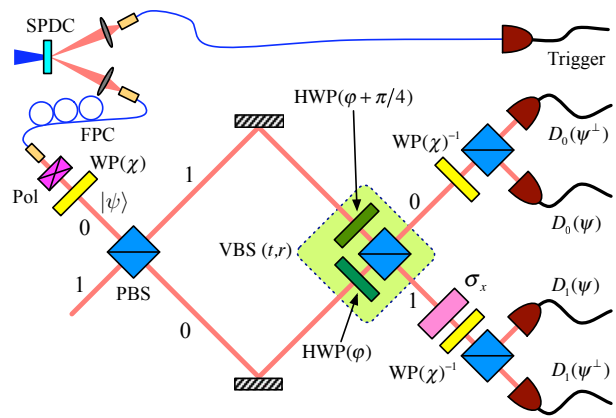


FIG. 2: Experimental setup. The heralded single-photon state was used to implement the postselection-free linear optical MDM device shown in Fig. 1. A fiber polarization controller (FPC), a vertical polarizer (Pol), and $WP(\chi)$ prepare the initial polarization qubit $|\psi\rangle$. $VBS(t, r)$ is realized by using a pair of HWP’s and a PBS.

system-ancilla two-qubit state and is found to be $\rho_F = |\psi'_0\rangle_{ss}\langle \psi'_0| + |\psi'_1\rangle_{ss}\langle \psi'_1|$ where $|\psi'_0\rangle_s = \alpha t|0\rangle_s + \beta r|1\rangle_s$ and $|\psi'_1\rangle_s = \alpha r|0\rangle_s + \beta t|1\rangle_s$. The operation fidelity which quantifies the overlap between the input state $|\psi\rangle_s$ and the output state ρ_F is defined as $F_\psi = {}_s\langle \psi | \rho_F | \psi \rangle_s$. As before, by averaging over all possible pure states on the Bloch sphere, the average operation fidelity becomes

$$F_{\text{avg}} = \int F_\psi d\psi = \frac{2}{3}(1 + tr). \quad (3)$$

Note that the measurement strength setting which is equal to the classical random guess, i.e., $t = r = 1/\sqrt{2}$, results in $F_{\text{avg}} = 1$. In other words, the system qubit has not been disturbed. Any stronger measurement, however, will reduce the average operation fidelity F_{avg} . By equating eq. (2) and eq. (3), we arrive at the trade-off relation between G_{avg} and F_{avg}

$$F_{\text{avg}} = \frac{2}{3} + \frac{\sqrt{1 - (6G_{\text{avg}} - 3)^2}}{3}, \quad (4)$$

which in fact is the exact minimum disturbance measurement condition in Ref. [9] for a qubit.

The actual experimental setup to realize the quantum circuit in Fig. 1 is schematically shown in Fig. 2. To prepare the single-photon state needed to implement the proposed MDM device, we employ the heralded single-photon source using spontaneous parametric down-conversion (SPDC) [14, 15]. The SPDC signal-idler photon pair was generated in a 3 mm thick type-II BBO crystal pumped by a frequency-doubled ultrafast pulses from a mode-locked Ti:Sapphire laser operating at 780 nm. The pump beam was focused on the BBO crystal with a lens ($f = 300$ mm) and the 780 nm signal-idler photon pair, emitted in the beam-like configuration at

$\pm 3.38^\circ$ with respect to the pump beam, was coupled into single-mode fibers using $\times 10$ objective lenses located at 650 mm from the crystal [16].

The idler photon was directly coupled to the trigger detector so that the detection signal can be used to herald the single-photon state for the signal photon. A fiber polarization controller (FPC) and a vertical polarizer (Pol) prepare the initial polarization state of the signal photon at $|V\rangle$. It is then transformed unitarily to an arbitrary polarization qubit $|\psi\rangle_s = \alpha|H\rangle_s + \beta|V\rangle_s$ using $\text{WP}(\chi)$, which consists of a HWP at an angle θ_1 followed by a QWP at an angle θ_2 . (The vertical polarization is defined to be 0° .) The ancilla path qubit, which is initialized at $|0\rangle_a$, is introduced to the same single-photon state by directing the photon at one (labeled as 0) of the two input modes of the PBS. The other input spatial mode of the PBS, labeled 1, is not used. For the prepared initial two-qubit state $|\psi\rangle_s \otimes |0\rangle_a$, the CNOT operation between the polarization qubit and the path qubit is implemented with the PBS [13, 17].

A balanced Mach-Zehnder interferometer with a variable beam splitter $\text{VBS}(t, r)$, which consists of a PBS and a HWP in each of the input modes of the PBS, then implements the Hadamard-like unitary transformation H' on the path qubit, i.e., creating arbitrary quantum superposition between the two orthonormal basis vectors $|0\rangle_a$ and $|1\rangle_a$ of the ancilla path qubit. The angle of HWP in path 0 is set at φ and the corresponding angle of the HWP in the path 1 is set at $\varphi + \pi/4$. The transmission and the reflection coefficients of the HWP-PBS system is then given as $t = \cos 2\varphi$ and $r = \sin 2\varphi$. Thus, by varying the HWP angle φ we can control the strength of measurement on the system (polarization) qubit. Note that the initial PBS, which implements the CNOT operation between the polarization qubit and the path qubit, and the second PBS, which implements H' operation on the path qubit, form a balanced Mach-Zehnder interferometer.

A single-photon emerging at the output mode 0 or 1 of $\text{VBS}(t, r)$ would then mean measurement of the path qubit with the outcome 0 or 1, respectively. We guess (or infer) that, if the measurement outcome of the path qubit is 0 or 1, the input polarization qubit must have been in the $|H\rangle$ or $|V\rangle$ state, respectively, with a certain fidelity. For a single-photon emerging at the output mode 0 of $\text{VBS}(t, r)$, i.e., the outcome of measurement on the ancilla path qubit is $|0\rangle$, the state of the system qubit (the polarization state) must be $\alpha t|H\rangle + \beta r|V\rangle$. Similarly, for a single-photon emerging at the output mode 1 of the HWP-PBS system, the polarization state must be $\beta t|H\rangle + \alpha r|V\rangle$. We thus apply the conditional feed-forward operation σ_x in the output mode 1 to flip the polarization state so that $|H\rangle \leftrightarrow |V\rangle$ and this operation was implemented with a HWP set at 45° . (Note that σ_z was needed for the protocol described in Fig. 1.)

Finally, to perform state analysis on the output system

qubit (the polarization state), we first apply the inverse polarization transformation $\text{WP}(\chi)^{-1}$ by using a QWP at an angle $\theta_2 + \pi/2$ followed by a HWP at an angle θ_1 , in each output mode of the Mach-Zehnder interferometer. The state of the output system qubit was then analyzed by using a PBS followed by two detectors, $D_i(\psi)$ and $D_i(\psi^\perp)$, at the output mode i of the Mach-Zehnder interferometer. Here, $\langle \psi | \psi^\perp \rangle = 0$. Keep in mind that the subscript i ($i = 0$ or 1) denotes the measurement outcome of the ancilla path qubit. Since we are dealing with the heralded single-photon source, we record the coincidence count between the trigger detector and one of the four detectors $D_i(\psi)$ and $D_i(\psi^\perp)$. Note that the coincidence measurement needed for heralded single-photon state has nothing to do with the postselection-free feature of the present MDM protocol.

The experimental estimation fidelity G_{avg} and the operation fidelity F_{avg} are obtained from the detection events as follows. First, the measurement strength on the ancilla path qubit was set by choosing the HWP angle φ between 0° and 22.5° . When $\varphi = 22.5^\circ$, H' becomes the usual Hadamard operation on the path qubit since $t = r = 1/\sqrt{2}$ and this corresponds to the weakest measurement or the classical random guess. The strongest measurement setting is $\varphi = 0^\circ$.

Second, for an input system qubit (the polarization state) $|\psi\rangle_s$, we measure the coincidence counts between the trigger detector and one of the four state analyzing detectors $D_i(\psi)$ and $D_i(\psi^\perp)$ while keeping the phase difference between the two arms of the Mach-Zehnder interferometer at 0, modulo 2π . Since the multi-mode fiber coupled detectors have slightly different coupling efficiencies, the raw coincidence counts are then corrected for the measured coupling efficiencies, resulting $N_i(\psi)$ and $N_i(\psi^\perp)$. The normalized count is defined as $n_i(\psi) = N_i(\psi)/N_{\text{tot}}$, where $N_{\text{tot}} = N_0(\psi) + N_0(\psi^\perp) + N_1(\psi) + N_1(\psi^\perp)$, and similarly for $n_i(\psi^\perp)$.

Third, the state dependent operation fidelity F_ψ is then evaluated as $F_\psi = \langle \psi | \rho_F | \psi \rangle = n_0(\psi) + n_1(\psi)$. The state dependent estimation fidelity is evaluated as

TABLE I: An experimental data set for $\varphi = 22.5^\circ$. Channel efficiency corrected coincidence counts (Hz), averaged over four independent measurements, are shown for six different input states. This data set is used to evaluate the G_{avg} and F_{avg} . This measurement is then repeated three times.

ψ	$N_0(\psi)$	$N_0(\psi^\perp)$	$N_1(\psi)$	$N_1(\psi^\perp)$
$ H\rangle$	71.72	0.48	73.73	0.40
$ V\rangle$	82.97	0.26	77.08	0.11
$ D\rangle$	77.69	0.67	78.07	2.31
$ A\rangle$	80.73	1.67	73.51	2.97
$ R\rangle$	78.07	1.33	74.16	4.95
$ L\rangle$	83.02	2.00	75.46	1.65

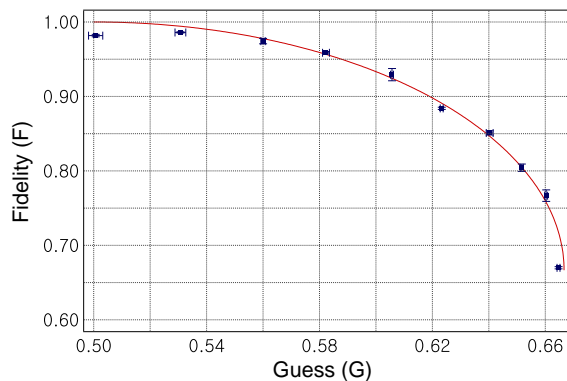


FIG. 3: Experimental data. Solid line shows the theoretical optimal trade-off relation between the information gain and the state disturbance due to measurement. The experimental estimation fidelity G_{avg} and the operation fidelity F_{avg} are shown as solid squares.

$G_\psi = \langle \psi | \rho_G | \psi \rangle = P_0 |\langle H | \psi \rangle|^2 + P_1 |\langle V | \psi \rangle|^2$, where the probability of measurement outcome of i is given as $P_i = n_i(\psi) + n_i(\psi^\perp)$. The state-dependent G_ψ and F_ψ are then obtained for six different input system qubits, i.e., $|H\rangle$, $|V\rangle$, $|L\rangle = (|H\rangle + i|V\rangle)/\sqrt{2}$, $|R\rangle = (|H\rangle - i|V\rangle)/\sqrt{2}$, $|D\rangle = (|H\rangle + |V\rangle)/\sqrt{2}$, $|A\rangle = (|H\rangle - |V\rangle)/\sqrt{2}$ [10]. The state-averaged estimation and operation fidelities G_{avg} and F_{avg} are then obtained by averaging G_ψ and F_ψ values, respectively, for the six input states. Finally, the whole procedure was repeated for 10 different settings of the measurement strength, i.e., 10 different angle settings of φ .

A sample of the experimental data is shown in Table I. The setting for the measurement, $\varphi = 22.5^\circ$, corresponds to the classical random guess, i.e., the theoretical estimation fidelity $G = 0.50$. The numbers correspond to channel efficiency corrected coincidence counts (Hz), averaged over four independent measurements, for six different input states. We perform three sets of measurements like in Table I to experimentally evaluate the estimation fidelity G_{avg} and the operation fidelity F_{avg} for each of the measurement setting.

The final experimental data are shown in Fig.3. The solid line shows the theoretical optimal trade-off relation of eq. (4) between the information gain (or classical guess; estimation fidelity) and the state disturbance due to measurement (operation fidelity). The experimental data are shown in solid squares and they summarize the results of three experimental runs. It is clear that the experimentally obtained G_{avg} and F_{avg} closely follow the MDM condition in eq. (4). Slightly less than ideal operation fidelity, i.e., $F < 1$, when the estimation fidelity $G = 0.5$ is due to the imperfect alignment of the Mach-Zehnder interferometer, imperfect optics, and small efficiency differences between the detectors. (To reach $F = 1$, the Mach-Zehnder interferometer would have to exhibit 100%

interference visibility.)

In summary, we have proposed a novel minimum disturbance measurement protocol and the corresponding postselection-free linear optical scheme to implement the protocol using the single-photon polarization-path two-qubit state. We have also demonstrated the proposed scheme using the heralded single-photon source from spontaneous parametric down-conversion, showing good agreement with the theoretical G - F bound for the optimal quantum measurement. Finally, it is interesting to note that the present protocol and scheme could be expanded to explore optimal quantum measurement bound for high-dimensional quantum states or qudits by using, for example, multi-path interferometric geometries to realize high-dimensional path qudits [18, 19].

This work was supported, in part, by the Korea Science and Engineering Foundation (R01-2006-000-10354-0), the Korea Research Foundation (KRF-2005-015-C00116 and R08-2004-000-10018-0), and by the Ministry of Commerce, Industry and Energy of Korea through the Industrial Technology Infrastructure Building Program.

-
- [1] A. Peres, *Quantum Theory: Concepts and Methods* (Kluwer, Dordrecht, 1995).
 - [2] W. Heisenberg, *The Physical Principles of the Quantum Theory* (Dover, New York, 1930).
 - [3] M.O. Scully and K. Drühl, *Phys. Rev. A* **25**, 2208 (1982).
 - [4] Y.-H. Kim *et al.*, *Phys. Rev. Lett.* **84**, 1 (2000).
 - [5] Similarly, quantitative analysis of the complementarity (the wave-particle duality) requires quantifying the concept of which-path information. See, W.K. Wothers and W.H. Zurek, *Phys. Rev. D* **19**, 473 (1979); L.S. Bartell, *ibid.*, **21**, 1698 (1980); B.-G. Englert, *Phys. Rev. Lett.* **77**, 2154 (1996); P.D.D. Schwindt, P.G. Kwiat, and B.-G. Englert, *Phys. Rev. A* **60**, 4285 (1999).
 - [6] S. Massar and S. Popescu, *Phys. Rev. Lett.* **74**, 1259 (1995).
 - [7] D. Bruss and C. Macchiavello, *Phys. Lett. A* **253**, 149 (1999).
 - [8] C.A. Fuchs and A. Peres, *Phys. Rev. A* **53**, 2038 (1996).
 - [9] K. Banaszek, *Phys. Rev. Lett.* **86**, 1366 (2001).
 - [10] F. Sciarrino *et al.*, *Phys. Rev. Lett.* **96**, 020408 (2006).
 - [11] T.B. Pittman, B.C. Jacobs, and J.D. Franson, *Phys. Rev. Lett.* **88**, 257902 (2002).
 - [12] U.L. Andersen *et al.*, *Phys. Rev. Lett.* **96**, 020409 (2006).
 - [13] Y.-H. Kim, *Phys. Rev. A* **67**, 040301(R) (2003).
 - [14] C.K. Hong and L. Mandel, *Phys. Rev. Lett.* **56**, 58 (1986).
 - [15] S.-Y. Baek, O. Kwon, and Y.-H. Kim, *Phys. Rev. A* **77**, 013829 (2008).
 - [16] Y.-H. Kim, *Phys. Rev. A* **68**, 013804 (2003).
 - [17] N.J. Cerf, C. Adami, and P.G. Kwiat, *Phys. Rev. A* **57**, R1477 (1998).
 - [18] G. Weihs *et al.*, *Opt. Lett.* **21**, 302 (1996).
 - [19] R.T. Thew *et al.*, *Phys. Rev. Lett.* **93**, 010503 (2004).